Depletion driven adsorption of colloidal rods onto a hard wall

Richard P. Sear*
FOM Institute for Atomic and Molecular Physics Kruislaan 407, 1098 SJ Amsterdam, The Netherlands
(Received 3 September 1997)

In a mixed suspension of rods and small polymer coils, the rods adsorb onto a hard wall in contact with the suspension. This adsorption is studied in the low density of rods limit. It is driven by depletion forces and is much stronger for long rods than for spheres. This is shown by means of exact, numerical, calculations and an approximate theory. [S1063-651X(98)08202-6]

PACS number(s): 82.70.Dd, 67.70.+n, 61.25.Hq

I. INTRODUCTION

Most of the properties of a colloidal suspension depend on the shape of its constituent particles. Certainly, the bulk phase behavior of colloidal particles is sensitive to their shape, as well as to the strength of any attractive interactions. Spheres behave differently from rods, which in turn behave differently from disks. This is true in the presence [1,2] and in the absence [3,4] of attractive interactions. However, a description of the bulk phase behavior does not complete the description of a suspension. We might also like to know, for example, its behavior near the walls of its container. We study this behavior here for rodlike colloidal particles in the presence of nonadsorbing polymer, and compare this behavior to that of spherical particles. A pure suspension of rods does not adsorb onto a hard wall, in the absence of significant van der Waals attractions; here we will assume that they are negligible. Indeed, the density of rods near the wall is below the bulk density. However, the rods in a mixed suspension of rods and small nonadsorbing (onto either the rods or the wall) polymer coils do adsorb onto the wall. This adsorption is driven by the increase in the volume available to the polymer coils when a rod is near a wall, the so-called depletion forces [5–9]. We find much stronger adsorption for rods than has been found for spheres [10–12].

The depletion driven adsorption of spherical colloidal particles onto a wall has been extensively studied [10–14]. These studies were primarily experimental but comparison was made with theories for depletion forces [15,16] and qualitative agreement found. Both the sphere and the wall exclude the centers of mass of the polymer coils from a volume that extends up to about the radius of gyration of the polymer away from the surface of the sphere or wall: the Asakura-Oosawa model for the interaction of the polymer with the sphere and wall [15,16]. This is true as long as the radius of gyration is not too much larger than the radius of the sphere [17]. When a sphere approaches the wall, the volume the sphere excludes to the polymer and the volume the wall excludes to the polymer overlap. Thus the total volume denied to the polymer coils goes down and so their translational entropy goes up. For polymer coils rather smaller than the spheres, free energies of adsorption of up to $6k_BT$ have been obtained [10,11], where k_B is Boltzmann's constant and T is the temperature.

Rodlike colloids are not uncommon, examples are the tobacco mosaic virus [18] and synthetic colloidal rods [9,19]. The effect of adding polymer to their suspensions has been studied, at least in the bulk [9,18,20]. As far as we are aware, no experiments comparable to those for spheres near a wall have been performed. However, Buitenhuis *et al.* [20] report a thin layer of the nematic phase of the rods against the wall of their capillary. This is at least suggestive of some attraction between the rods and the capillary. The adsorption of rods does not seem to have been much studied theoretically. An exception is the work of Matsuyama *et al.* [21], who studied a model of rods with discrete orientations. However, the adsorption of polymers that have some degree of rigidity has been studied; see Ref. [22] and references therein. The results are consistent with those found here; as the rigidity of the polymer increases, so does the adsorption.

In the following section we first derive the exact statistical mechanical expression for the density profile of rods near a wall, as a function of the polymer density. We use this expression in two ways: the first is by evaluating it exactly using Monte Carlo integration and the second is by deriving a simple analytical approximation to it. Example profiles of the density of rods near the wall are shown and discussed in Sec. III. We end with a conclusion, Sec. IV.

II. THEORY

We start by defining our models for the rod, the polymer coil, and the wall. The interactions between polymer coils are neglected, i.e., a fluid of just polymer coils is simply an ideal gas. This leaves us with just three interactions in order to describe our system: the rod-wall, polymer-wall, and rod-polymer interactions. The rod-wall interaction is that of a hard spherocylinder with a smooth hard wall. The spherocylinder is of length l and diameter $d=2r_c$. Thus, no point on the center line of the rod, a line of length l that runs along the center of the cylindrical portion of the spherocylinder, may be within r_c of the wall; see Fig. 1(a). Note that, as usual [23], the length l is the length of the cylindrical part of the spherocylinder; its total length is $l+d$. For the purposes of the polymer-wall and polymer-rod interactions, a polymer

*Present address: Department of Chemistry and Biochemistry, The University of California at Los Angeles, 405 Hilgard Avenue Los Angeles, CA 90095-1569.

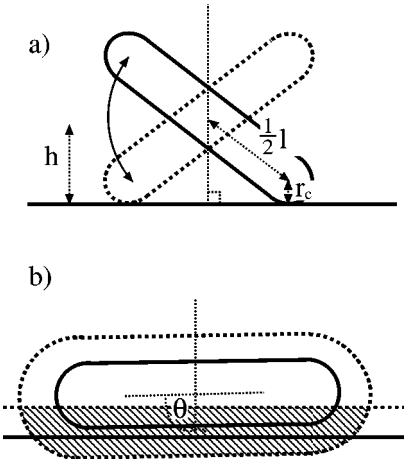

FIG. 1. Schematics of a hard spherocylinder near a hard wall. (a) The solid spherocylinder shows it at the smallest angle possible without overlap of the spherocylinder with the wall and the dashed spherocylinder shows it the largest angle. The solid arc with arrows denotes the range of angles available to the spherocylinder at that height. (b) The cross section of the overlap of the volume a rod excludes to the polymer with the volume the wall excludes to the polymer is shown as the shaded area. The solid lines are the surface of the spherocylinder and the wall, and the dashed lines are the surfaces of the volumes they exclude to the polymer.

coil is considered to be a hard sphere of radius r_p; this is the so-called Asakura-Oosawa model [15,16,24,25]. Then the position of a polymer coil is entirely determined by the position of its center of mass. This center of mass is prevented from coming within r_p of the wall and from r_p+r_c from any point on the center line of the rod. The rod excludes polymer molecules from a spherocylindrical volume of length l and diameter $2(r_c+r_p)$.

Now that we have defined our model we write down the partition function Ξ for a system of one colloidal rod and a fluid of polymer molecules at an activity z_p,

$$\Xi=\sum_{N_p}\frac{z_p^{N_p}}{N_p!}\int d\mathbf{r}\,d\omega\,d\mathbf{r}^{N_p}\exp[-\beta u_{rw}(\mathbf{r},\omega)]\times\prod_{i=1,N_p}\exp[-\beta u_{pw}(\mathbf{r}_i)-\beta u_{rp}(\mathbf{r},\omega,\mathbf{r}_i)],\qquad(1)$$

where the coordinates of the center of mass of the rod are denoted by $\mathbf{r}$, and its orientation by ω. The coordinates of all N_p polymer coils are denoted by $\mathbf{r}^{N_p}$ and the coordinates of the ith polymer coil by $\mathbf{r}_i$. As usual β is related to the temperature T by $\beta=1/k_BT$. The polymer's activity z_p is related to its chemical potential μ_p by $z_p=\Lambda^{-1}\exp(\beta\mu_p)$, where Λ is the thermal volume of a polymer coil. u_{rw}, u_{pw}, and u_{rp} are the energies of interaction of the rod with the wall, a polymer molecule with the wall, and the rod with a polymer molecule, respectively. They are all hard-core interactions and so are zero unless the particles overlap, in which case they are infinite. As there are no polymer-polymer interactions, Eq. (1) simplifies to

$$\Xi=\int d\mathbf{r}\,d\omega\,\exp[-\beta u_{rw}(\mathbf{r},\omega)]\times\sum_{N_p}\frac{z_p^{N_p}}{N_p!}\left(\int d\mathbf{r}_1\exp[-\beta u_{pw}(\mathbf{r}_1)-\beta u_{rp}(\mathbf{r},\omega,\mathbf{r}_1)]\right)^{N_p}.\qquad(2)$$

The integrand of the part of Eq. (2), which is within parentheses, is 0 if the polymer sphere is within r_p of either the wall or the surface of the spherocylinder and 1 otherwise. Therefore, the integral within parentheses is equal to the volume of the system, which is farther than r_p from both the wall and the rod's surface, the free volume for the polymer $V_f(\mathbf{r},\omega)$. If in addition we recognize the sum of Eq. (2) as being just the expansion of an exponential function, we have

$$\Xi=\int d\mathbf{r}\,d\omega\,\exp[-\beta u_{rw}(\mathbf{r},\omega)+z_pV_f(\mathbf{r},\omega)].\qquad(3)$$

The volume V_f may be written as a sum of three parts,

$$V_f(\mathbf{r},\omega)=V_b-v_{\rm exc}+v_0(\mathbf{r},\omega),\qquad(4)$$

where V_b is the total volume available to a polymer in the absence of the rod and $v_{\rm exc}=\pi lr_e^2+(4/3)\pi r_e^3$, the volume excluded by the rod to the polymer molecules; $r_e=r_c+r_p$, the radius of the excluded volume spherocylinder around a rod. v_0 is the volume of overlap of the volume excluded to the polymer by the rod and the volume excluded to the polymer by the wall; see Fig. 1(b). Thus if the rod is far from the wall then the regions excluded to the polymer by the rod and by the wall do not overlap and $v_0=0$ but if the rod is close to the wall then these two excluded volumes overlap and so $v_0>0$. The total volume available to the polymer has increased. It is this increase in the free volume, or to put it another way, the reduction in the volume excluded to the polymer, which is the driving force for adsorption of the rod onto the wall. The adsorption is not driven by a direct rod-wall interaction as is usually the case. Using Eq. (4) we can rewrite Eq. (3) as

$$\Xi=\exp[z_p(V_b-v_{\rm exc})]\times\int d\mathbf{r}\,d\omega\,\exp[-\beta u_{rw}(\mathbf{r},\omega)+z_pv_0(\mathbf{r},\omega)].\qquad(5)$$

As the wall is smooth both u_{rw} and v_0 are functions only of the angle between the surface normal and the axis of the rod, θ, and of the distance between the center of mass of the rod and the nearest point of the wall, h.

Now that we have integrated over the polymer coordinates, Ξ is a one particle partition function and so the probability of finding the rod at coordinates (h,θ) is proportional to the integrand of Eq. (3). We now consider an ideal gas of rods, i.e., rods at a density so low that interactions between the rods have a negligible effect. Then the rods are independent of each other and the density of rods $\rho(h,\theta)$ is again proportional to the integrand of Eq. (3),

$$\rho(h,\theta)=\rho_b\exp[-\beta u_{rw}(h,\theta)+z_pv_0(h,\theta)],\qquad(6)$$

where ρ_b is the bulk density of the ideal gas of rods. In the absence of polymer, Eq. (6) yields a density proportional to the Boltzmann weight; with polymer present, its entropy, times $-k_BT$, acts as an additional ''energy'' in the Boltzmann weight. Equation (6) is exact in the low density of rods limit and is the equation we will use to determine how strongly the rods adsorb onto the surface, in the presence of the polymer. We are interested in the h, not the angle dependence of the density of rods, and so we integrate Eq. (6) over θ:

$$\rho(h)=\rho_b\,\frac{1}{2}\int_{-1}^{1} d(\cos\theta)\exp[-\beta u_{rw}(\mathbf{r},\theta)+z_p v_0(\mathbf{r},\theta)], \tag{7}$$

where the factor of a half is the normalization of the integration over θ. Note that Eq. (7) has exactly the same form for rods near a wall with a direct rod-wall attractive interaction; the term $-z_p k_B T v_0(\mathbf{r},\theta)$ is an effective rod-wall attractive interaction. It is attractive because if the rod is far from the wall $v_0=0$ and then as the rod nears the wall v_0 becomes positive, thus tending to increase the density of rods. Equation (7) is directly related to the change in free energy $\Delta F(h)$ when a rod is brought from within the bulk to a height h:

$$\Delta F=-k_BT\,\ln(\rho(h)/\rho_b). \tag{8}$$

This quantity has actually been measured experimentally for spheres [10,11]. As all the interactions are athermal the energy is zero and the free energy ΔF is simply an entropy times T. Finally, from Eq. (7) the adsorption Γ is easily calculated using [26]

$$\Gamma=\int_0^\infty dh[\rho(h)-\rho_b]. \tag{9}$$

A. Rod near a wall

It is instructive to consider just a hard spherocylinder near a hard wall; the $z_p=0$ limit of Eq. (7). The potential u_{rw} is zero as long as the rod and wall do not overlap. For this to be true the lowest point of the center line must be at least r_c above the wall, as the surface of the spherocylinder is r_c away from the center line. The lowest point of the center line of the spherocylinder is always one of its two ends; see Fig. 1(a). Therefore, u_{rw} is zero providing both ends of the center line are at least r_c above the wall and is infinity otherwise. Then, for $z_p=0$, we can perform the integration over θ of Eq. (7), to obtain the density of spherocylinders as a function of height:

$$\rho(h)=\begin{cases}\rho_b 2(h-r_c)/l, & (h-r_c)\leqslant l/2\\ \rho_b, & (h-r_c)>l/2.\end{cases} \tag{10}$$

The density of centers of mass of the spherocylinders decreases linearly as the wall is approached due to the restricted orientations of a rod close to a wall.

B. Numerical evaluation of v_0

The overlapping excluded volume $v_0(h,\theta)$ is the volume of overlap of a spherocylinder of length l and radius r_e with a half-space. We evaluate it numerically using a Monte Carlo integration scheme [27]. Briefly, first a randomly located point within the spherocylinder is generated, in a coordinate frame fixed on the spherocylinder. Generating a point within a spherocylinder is done by first selecting either the cylindrical part or the end caps. The probability of selecting the cylinder (end caps) is given by the fraction of the total volume of the spherocylinder, which is part of the cylinder (end gaps). In the cylindrical part, the point's coordinate along the axis is just a random number between $-l/2$ and $l/2$ and its coordinates perpendicular to the axis are those of a random point within a disk. In the end caps the point is obtained by first generating a random point within a sphere. Then if the coordinate of this point along the axis of the spherocylinder is positive $l/2$ is added to it and if it is negative $l/2$ is subtracted. Generating a point randomly within a sphere or disk is done with a routine of Appendix G of Ref. [28]. Now we have a randomly chosen point within the spherocylinder, in a frame fixed on the spherocylinder. The spherocylinder is then rotated to an angle of θ with the normal of the wall. If the point's height above the wall is then less than r_p then it is within that part of the volume excluded by the spherocylinder, which is also excluded by the wall and hence is part of v_0. If it is above r_p it is not. If many such points are generated then the fraction of points that lie below r_p is an approximation to the fractional overlap $v_0(h,\theta)/v_{\rm exc}$.

C. Approximate theory

Here we derive a simple analytical approximation for $\rho(h)$. In the presence of polymer the highest density of rods will be near to the wall, as then v_0 is largest. Therefore, an approximation should be accurate in this region. The volume

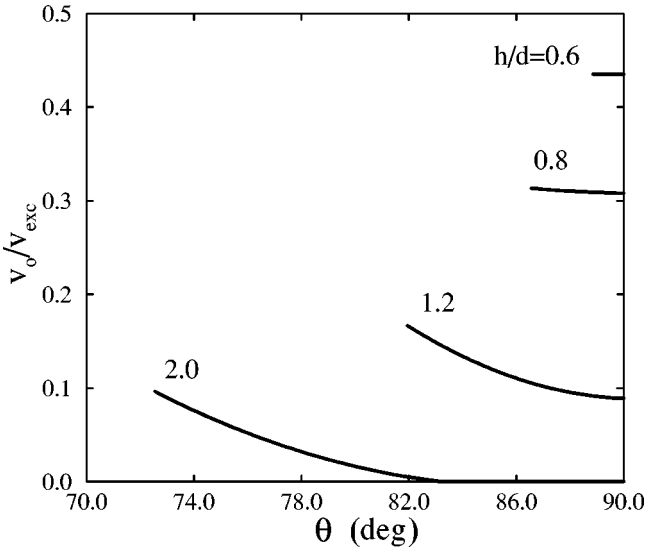

FIG. 2. The fraction of the volume excluded by the rod which overlaps with that of the wall, as a function of θ (in degrees) for several values of h/d. Each curve is labeled by the value of h/d. For all curves, $l/d=10$ and $r_p=r_c$. The curves are plotted over the range in θ for which the hard core of the spherocylinder does not overlap with the wall.

v_0 is quite small, a fraction of r_e^3, if the angle θ is small, i.e., the rod is nearly perpendicular to the wall. However, v_0 is large, a fraction of lr_e^2, if the rod is nearly parallel to the wall and close to it, $h<r_e+r_p$. This is assuming that $l \gg r_e$. In fact as v_0 appears as the argument of the exponential function in Eq. (7) for the density, the density of rods close and nearly parallel to the wall increases as exp(l). As we shall see in the next section this can lead to very strong adsorption.

So, we require an approximation accurate for rods close to, and hence necessarily almost parallel to, the wall. In Fig. 2 we have plotted v_0/v_{exc} as a function of θ for a number of heights h. For small h the spherocylinder is restricted to a small range of angles by the hard-core spherocylinder-wall interaction. In addition v_0 is not a strongly varying function of θ, especially near the wall. Therefore, we approximate v_0 for the whole range of accessible values of θ by its value for $\theta=90°$. Then, our approximate expression for $\rho(h)$ is

$$\rho(h)=\begin{cases} \rho_b \dfrac{2(h-r_c)}{l} \exp[z_p v_0(h,90°)], & (h-r_c) \leqslant l/2 \\ \rho_b, & (h-r_c) > l/2. \end{cases} \tag{11}$$

$v_0(h,90°)$ is easy to calculate. It consists of two parts, the volume of the cylinder of radius r_e at a height h, which is below a height of r_p, and the volume of a sphere of the same radius, which is below this height. So,

$$v_o(h,90°)=\begin{cases} l\left[r_e^2 \cos^{-1}\left(\frac{h-r_p}{r_e}\right) \right. \\ \left. -(h-r_p)\left(r_e^2-(h-r_p)^2\right)^{1/2}\right] \\ +\frac{\pi}{3}\left[2r_e^3-3r_e^2(h-r_p)\right. \\ \left.+(h-r_p)^3\right] & h \leq r_e+r_p \\ 0 & h > r_e+r_p. \end{cases} \tag{12}$$

Equation (12) is restricted to $r_c \geqslant r_p$ and so requires generalization if $r_p>r_c$. However, the Asakura-Oosawa model [8,15,16] of the rod-polymer interaction is best for small polymer coils, with a radius of gyration no larger than that of the colloidal particle [16,17,29]. Therefore, we will not perform calculations with $r_p>r_c$ and so do not require a more general expression.

For $h>r_e+r_p$, $v_0(h,90°)=0$ and the approximation of Eq. (11) yields the same value for $\rho(h)$ as in the absence of polymer, Eq. (10). However, for small and large (near π) θ's v_0 is still nonzero (see Fig. 2) and so Eq. (11) is an underestimate. As h approaches r_c the arc over which the rod may rotate tends to zero and then the approximation of Eq. (11) becomes increasingly accurate. For small r_p the rod must be quite close for the excluded volume of a near parallel rod to overlap with that of the wall. So, reducing r_p will improve the accuracy of Eq. (11). Also, if l is large then the arc over which the rod can rotate decreases and so our approximation becomes more accurate. In the opposite limit: $l \to 0$, the approximation of Eq. (11) is exact; as it is in the $z_p=0$ limit.

III. RESULTS AND DISCUSSION

Now we are able to calculate the density of rods near a wall both exactly via the numerical technique of Sec. II B and via the simple approximate theory of Sec. II C. We have done so for a number of different values of the length to diameter ratio l/d of the rods, and the activity of the rods z_p. A dimensionless polymer activity is required; we define the reduced activity $z=z_p(2r_p)^3$. As there are no polymer-polymer interactions and the density of rods is so low that they take up a negligible fraction of the volume, the density of polymer coils is equal to their activity z_p [8,9]. So, the volume fraction occupied by the coils is $(\pi/6)z \simeq (1/2)z$. In Figs. 3 and 4, we show how the density of the centers of mass of rods near the wall depends on their length and on the concentration of the polymer. Note that Fig. 3 is for a polymer coil of radius half that of the rod while Fig. 4 is for polymer coils with the same radius as the rod. The free energy change on bringing a rod from within the bulk to a height h is proportional to $-\ln\rho(h)$, see Eq. (8). The adsorption Γ is plotted in Fig. 5.

Both the exact numerical integration of Eq. (7) over θ and the approximate Eq. (11) are shown in Figs. 3 and 4. The approximation is seen to be excellent near the peak in $\rho(h)$. The highest density of rods occurs only a little more than r_c above the wall, where the overlap of the excluded volumes is largest and the orientations of a rod are very restricted. This finding provides support for the related approximations made

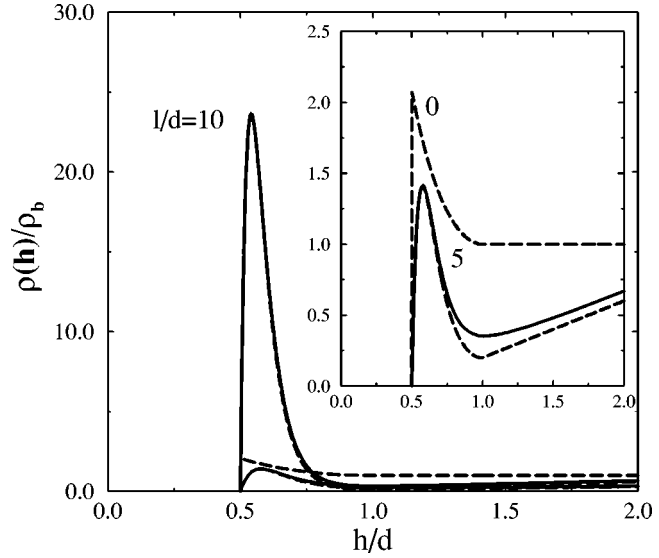

FIG. 3. The ratio of the density of rods $\rho(h)$ to their bulk density ρ_b, as a function of height h above the wall. The two solid curves are from Monte Carlo integration, the three dashed curves are from the analytical theory. The curves are labeled with their value of l/d; the dashed curve labeled 0 is for spheres. For all curves, $r_p=0.5r_c$ and $z=0.2$. The inset graph is an enlargement of a small region of the main graph.

in Ref. [2]. As can be seen in Fig. 2 v_0 varies very little over the restricted range of orientations available to a rod close to the wall. This makes our approximation almost indistinguishable from the exact, numerical result at these heights. Unlike spheres, the maximum in ρ is not at $h=r_c$. As h decreases, the orientational freedom of the rod decreases, see Eq. (10), and this tends to counterbalance the depletion attraction of the rod for the wall. In the $h\rightarrow r_c$ limit the orientational freedom of a rod tends to 0 and so the density of rods tends to 0. The approximation is much less good near the minimum in $\rho(h)$, which is to be expected as there the rods can rotate over a much larger angle. The approximation consistently underestimates $\rho(h)$ because it underestimates v_0. As can be seen in Fig. 2, v_0 is a minimum for $\theta=90°$.

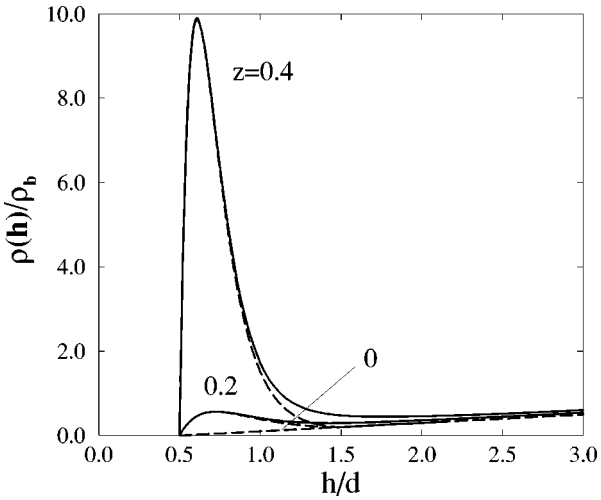

FIG. 4. The ratio of the density of rods $\rho(h)$ to their bulk density ρ_b, as a function of height h above the wall. The two solid curves are from Monte Carlo integration, the three dashed curves are from the analytical theory. The curves are labeled with their value of z. For all curves, $r_p=r_c$ and $l/d=10$.

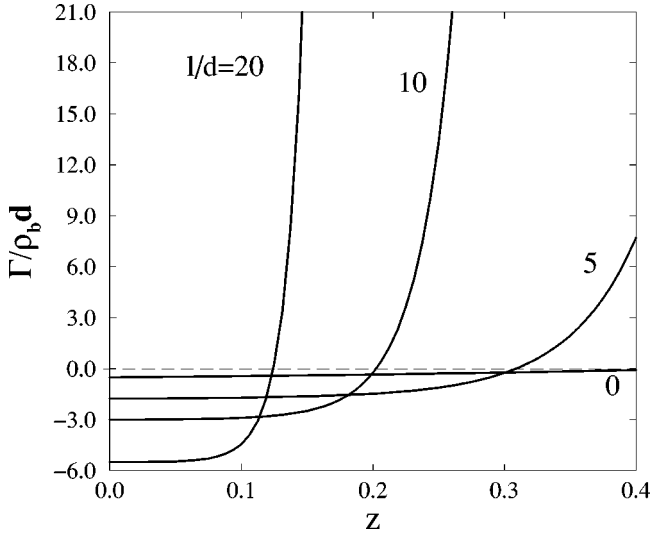

FIG. 5. The adsorption Γ is plotted as a function of z. Each curve is labeled with its value of l/d. The curve labeled 0 is for spheres. For all curves, $r_p=0.5r_c$.

From Fig. 3 it is clear that, in the presence of polymer, long rods, $l/d=10$, adsorb much more strongly onto a hard wall than do spheres. In Fig. 3 the maximum density of spheres is only about twice that in the bulk. However, the density of rods reaches a maximum of over 20 times the bulk value. For even longer rods the density maximum increases exponentially and becomes very large. The larger density maxima correspond to free energies of adhesion to the wall, which are many times k_BT; rods much longer than $l/d=10$ will adhere to the wall effectively irreversibly. The sensitivity of the adsorption to the length of the rod is also notable at small lengths. In Fig. 3 we see that, for this value of z, the density of short, $l/d=5$, rods is actually less than that of spheres. As rods, but not spheres, approach a wall they lose orientational entropy, which tends to reduce the density of the rods. Thus, without polymer the density of rods but not of spheres is reduced near a wall; see Eq. (10). For long rods and high z this is more than counterbalanced by the greater excluded volume of rods as compared to spheres. As z is increased beyond the value of 0.2 the density of $l/d=5$ rods near the wall increases more rapidly than that of spheres, and eventually becomes larger than that of spheres.

The dependence of the adsorption on the relative radii of the rod and of the polymer may be seen if Figs. 3 and 4 are compared. Figure 4 shows the density for rods with $l/d=10$ and polymer of the same radius, $r_p=r_c$, while Fig. 3 shows the density of rods with the same l/d and the same $z=0.2$ but with polymer of radius half that of the rod, $r_p=0.5r_c$. Of course, although the volume fraction of polymer is the same in each case, the number density of the smaller polymer is 8 times that of the larger. If the polymer's radius is the same as that of the rod then for $z=0.2$, which corresponds to a volume fraction of about 10%, the adsorption is very weak; the density near the wall is always less than that in the bulk. However, the same volume fraction of polymer of half the radius of the rods induces quite strong adsorption, a maximum density over 20 times the bulk density.

The adsorption Γ, calculated using Eq. (9), is plotted in Fig. 5, as a function of z for a number of values of l/d. The curves were calculated using the approximate expression for $\rho(h)$, Eq. (11). For the calculation of the adsorption Γ our approximation is highly accurate as it is accurate where the density is highest. This is particularly so at high z or l, the density in the peak near the wall grows exponentially with increasing z or l, see Eq. (11). Then the adsorption is dominated by this peak. It is obvious from Fig. 5 that the adsorption of long rods is very strong, or equivalently that only small volume fractions of polymer are required to produce a layer of rods near the wall with a much higher density than in the bulk.

IV. CONCLUSION

In a mixed suspension of rods and small polymer coils, the rods adsorb onto a hard wall in contact with the suspension. The adsorption is driven by depletion forces: The entropy of the polymer coils goes up when the rods lie close to and parallel to the wall. From Figs. 3 and 4 we see that the density of rods has a narrow peak, which implies that a monolayer is formed. This is expected as the depletion forces are short ranged. The rod feels the wall up to $l/2+r_c+2r_p$ away but the interaction is only strong when the rod approaches to within r_c+2r_p. Only then is there strong overlap of the excluded volumes. This is reflected in the density profile. Just at the surface there is a dense monolayer of rods lying parallel to the wall, then at larger separations the density of rods is actually below that of the bulk. The peak in the density is strongly dependent on l; longer rods adsorb strongly onto the wall. Again this is unsurprising, the excluded volume and hence the potential increase in the entropy of the polymer coils increases linearly with the length of the rod.

If we compare rods with spheres, we see that in the absence of polymer the density of rods but not of spheres drops as the wall is approached. This is due to the decrease in orientational freedom as a rod approaches a wall. In the presence of polymer, the larger excluded volume of a rod as compared with a sphere (if they have the same radius) causes the density of rods near the wall to increase more quickly than that of rods. The density of long rods becomes much higher near the wall than does the density of spheres.

Equation (6) for the density has exactly the same form for a rod attracted to the wall by a direct rod-wall interaction. So, in the presence of any attraction with a range approximately equal to the diameter of the rod, the density profiles will be qualitatively the same as those of our Figs. 3 and 4. This applies to, for example, van der Waals attractions [1,2].

So far, we have only considered an ideal gas of rods adsorbing onto a wall. This was reduced to a simple one-particle problem, which, of course, did not show a phase transition. Although we will not perform any calculations that account for interactions between rods at the wall it is, perhaps, interesting to speculate on what will happen near the wall. We have seen that the density near the wall can become much higher than that in the bulk, particularly if l/d is large. The density peak is narrow due to the short ranged attraction and so only a monolayer is formed. So, we expect a dense monolayer, which would resemble a system of two-dimensional rods. For strong adsorption the density of this monolayer will be much higher than in the bulk. This immediately suggests that even at low bulk densities, i.e., densities below a bulk transition to a nematic phase [23] or between two fluid phases [25,30], the density of a monolayer just above the wall may be high enough for this monolayer to undergo a transition to a two-dimensional nematic phase [3,21,31]. We expect the surface layer to be in the nematic phase for densities Γ of order $1/ld$ and greater. Crystallization of spheres at a wall at lower bulk densities than required for bulk crystallization has been observed [13] and treated theoretically [32].

ACKNOWLEDGMENTS

It is a pleasure to acknowledge a careful reading of the manuscript by J. Doye. I would like to thank The Royal Society for financial support and the FOM Institute AMOLF for its hospitality. The work of the FOM Institute is part of the research program of FOM and is made possible by financial support from the Netherlands Organization for Scientific Research (NWO).

[1] P. van der Schoot and T. Odijk, J. Chem. Phys. **97**, 515 (1992).
[2] R. P. Sear, Phys. Rev. E **55**, 5820 (1997).
[3] D. Frenkel, in *Liquids, Freezing and Glass Transitions,* Les Houches Course No. I, edited by J.-P. Hansen, D. Levesque, and J. Zinn-Justin (North-Holland, Amsterdam, 1991).
[4] M. P. Allen, G. T. Evans, D. Frenkel, and B. M. Mulder, Adv. Chem. Phys. **86**, 1 (1994).
[5] A. P. Gast, C. K. Hall, and W. B. Russell, Faraday Discuss. Chem. Soc. **76**, 189 (1983).
[6] H. N. W. Lekkerkerker, W. C. K. Poon, P. N. Pusey, A. Stroobants, and P. B. Warren, Europhys. Lett. **20**, 559 (1992).
[7] W. B. Russel, D. A. Saville, and W. R. Schowalter, *Colloidal Dispersions* (Cambridge University Press, Cambridge, 1989).
[8] W. C. K. Poon and P. N. Pusey, in *Observation, Prediction and Simulation of Phase Transactions in Complex Fluids*, Proceedings of the International School of Physics ''Enrico Fermi,'' Course CXXIX, edited by M. Baus, L. F. Rull, and J. P. Ryckaert (Kluwer, Dordrecht, 1995).
[9] H. N. W. Lekkerkerker, P. Buining, J. Buitenhuis, G. J. Vroege, and A. Stroobants, in *Observation, Prediction and Simulation of Phase Transactions in Complex Fluids,* Ref. [8].
[10] P. D. Kaplan, L. P. Faucheux, and A. J. Libchaber, Phys. Rev. Lett. **73**, 2793 (1994).
[11] D. L. Sober and J. Y. Walz, Langmuir **11**, 2352 (1995).
[12] A. D. Dinsmore, A. G. Yodh, and D. J. Pine, Nature (London) **383**, 239 (1996).
[13] P. D. Kaplan, J. L. Rourke, A. G. Yodh, and D. J. Pine, Phys. Rev. Lett. **72**, 582 (1994).
[14] Y. N. Ohsima *et al.*, Phys. Rev. Lett. **78**, 3963 (1997).
[15] S. Asakura and F. Oosawa, J. Chem. Phys. **22**, 1255 (1954).

[16] A. Vrij, Pure Appl. Chem. **48**, 471 (1976).
[17] E. Eisenriegler, A. Hanke, and S. Dietrich, Phys. Rev. E **54**, 1134 (1996).
[18] S. Fraden, in *Observation, Prediction and Simulation of Phase Transactions in Complex Fluids*, Ref. [8].
[19] P. A. Buining, A. P. Philipse, and H. N. W. Lekkerkerker, Langmuir **10**, 2106 (1994).
[20] J. Buitenhuis, L. N. Donselaar, P. A. Buining, A. Stroobants, and H. N. W. Lekkerkerker, J. Colloid Interface Sci. **175**, 46 (1995).
[21] A. Matsuyama, R. Kishimoto, and T. Kato, J. Chem. Phys. **106**, 6744 (1997).
[22] C. C. van der Linden, F. A. M. Leermakers, and G. J. Fleer, Macromolecules **29**, 1172 (1996).
[23] G. J. Vroege and H. N. W. Lekkerkerker, Rep. Prog. Phys. **55**, 1241 (1992).
[24] P. B. Warren, J. Phys. (France) I **4**, 237 (1994).
[25] H. N. W. Lekkerkerker and A. Stroobants, Nuovo Cimento D **16**, 949 (1994).
[26] J. R. Rowlinson and B. Widom, *Molecular Theory of Capillarity* (Clarendon Press, Oxford, 1982).
[27] W. H. Press, S. A. Teukolsky, W. T. Vetterling, and B. P. Flannery, *Numerical Recipes*, 2nd ed. (Cambridge University Press, Cambridge, 1992).
[28] M. P. Allen and D. J. Tildesley, *Computer Simulations of Liquids* (Clarendon Press, Oxford, 1987).
[29] R. P. Sear, J. Phys. (France) II **7**, 877 (1997).
[30] P. G. Bolhuis, A. Stroobants, D. Frenkel, and H. N. W. Lekkerkerker, J. Chem. Phys. **107**, 1551 (1997).
[31] Z. G. Wang, J. Phys. (France) **51**, 1431 (1990).
[32] W. C. K. Poon and P. B. Warren, Europhys. Lett. **28**, 513 (1994).